Thermal behaviour of weathered and consolidated marbles

J. RUEDRICH, T. WEISS & S. SIEGESMUND
Geowissenschaftliches Zentrum der Universität Göttingen, Goldschmidtstrasse 3, 37077 Göttingen, Germany (e-mail: jruedri@gwdg.de)

Abstract: To optimize stone consolidation it is necessary to understand the mechanisms of weathering in marbles, and its control by the mineralogical composition and the rock fabric. A knowledge of how the stone consolidants affect the weathering mechanisms and if they are compatible with the stone is also an important consideration. The weathering of marble can begin with thermal stress whereby cracks are generated. To verify whether consolidation influences the thermal behaviour of marbles, we compared the behaviour of weathered and consolidated marbles. For the investigations four marbles were selected with various fabrics (e.g. texture, grain size, grain boundary geometry, etc.) and different weathering conditions. Three consolidation approaches were adopted: a solved polymethyl-methacrylate ($PMMA_{sol}$) dissolved in xylenes, a polysilicic acid ester (PSAE) and a total impregnation with a monomer methyl-methacrylate ($PMMA_{poly}$). Measurements of the porosity and effective pore size distribution evidenced a strong modification of the pore space by consolidation. Both PMMA approaches show a re-establishment of cohesion which can be determined by ultrasonic velocity measurements. By reaching the respective glass transition temperatures of $PMMA_{sol}$ and $PMMA_{poly}$, a strong modification of thermal behaviour occurs. The PSAE consolidated marbles show only minor changes of dilatation, but due to its low bonding effect no significant cohesion between the crystals occurs.

For over a century stone consolidants have been extensively used for conservation purposes to save deteriorated natural building stones. Although a huge quantity of knowledge exists about consolidation, the selection of an appropriate impregnation material is still largely based on empirical considerations. If a consolidant appears to give acceptable results with one type of stone, it is often applied to other stone types, without properly determining if the consolidant is compatible with them. Some of the factors affecting the performance of consolidants are known, such as penetration depth and moisture transfer through consolidated stone. However, only a few considerations have been given to other important factors, e.g. compatibility of their thermal properties with the rock mineralogy and the rock fabric (cf. Clifton 1980).

Thermal dilatation processes are responsible for the initial degradation of marbles. Kessler (1919) found that repeated heating of marbles may lead to permanent dilatations due to microfracturing and that thermally treated marbles show a remarkable non-reversible change in length especially during the first heating cycle (Sage 1988; Tschegg *et al.* 1999; Siegesmund *et al.* 2000). Even small temperature changes of 20°C to 50°C may result in damage (Battaglia *et al.* 1993). Marble has a very simple mineralogical composition. It consists of calcite and/or dolomite with other accessory phases (e.g. quartz, mica etc.). Calcite and dolomite exhibit a pronounced anisotropy of the thermal expansion coefficient at different crystallographic directions (Kleber 1959) leading to stresses within the sample during heating. When these stresses exceed the threshold of cohesion a thermally induced deterioration is observed (cf. Sage 1988). The rock fabric, which includes grain size, grain aspect ratios, grain shape preferred orientation, lattice preferred orientation (texture) and the microcrack populations, significantly controls the material's behaviour during thermal stress (e.g. Siegesmund *et al.* 1997).

At present little is known concerning the manner or degree of change of thermoelastic properties upon impregnation. Siegesmund *et al.* (1999) observed an increase of directional dependence of the thermal expansion coefficient for samples of Wunsiedel marble impregnated with PMMA. However, this specimen was relatively unweathered which means that the rock's structure was more or less intact (i.e. good cohesion between the grains and low porosity).

In contrast, this paper investigates the influence of impregnation materials on thermal behaviour of weathered marbles with a special regard to the interaction between rock fabric and stone consolidant. Four marbles with different fabrics were selected: Carrara, Lasa, Sterzing (Italy) and Prieborn (Poland). Detailed

From: SIEGESMUND, S., WEISS, T. & VOLLBRECHT, A. 2002. *Natural Stone, Weathering Phenomena, Conservation Strategies and Case Studies*. Geological Society, London, Special Publications, **205**, 255–271.
0305-8719/02/$15.00

fabric analyses were performed on each sample. These marbles had been outside for different time spans, and therefore represent very different weathering conditions. The samples from Lasa, Sterzing and Prieborn show an intermediate decay, whereas the Carrara specimen is strongly deteriorated.

Marble samples were impregnated with the following consolidants: polymethyl-methacrylate ($PMMA_{sol}$) dissolved in xylenes, a polysilicic acid ester (PSAE) and methyl-methacrylate ($PMMA_{poly}$) polymerized within the marble. Thermal expansion measurements were carried out on both weathered and consolidated samples and the degradation by heat treatment was determined by ultrasonic velocity measurements. Moreover, porosity and pore size distribution analyses were used to characterize the intruded volume of consolidant and the occupied pore radii classes.

Analytical methods

A reference coordinate system for the investigations, with respect to the macroscopically visible elements of foliation and lineation (Fig. 1a) was chosen. The XY-plane marks a metamorphic foliation while the X-direction is parallel to the lineation. An arbitrary coordinate system was defined, if the specimens did not show any macroscopically visible fabric elements.

Petrographic analyses (in polarized light) on standard thin sections were performed for a qualitative description of different grain parameters (e.g. mineralogical composition, grain boundary geometry, microcrack systems). Quantitative values for different fabric parameters (grain size, grain boundary orientation etc.) were obtained from digital image analyses (Duyster 1991).

Scanning electron microscopy (SEM) on fractured surfaces (fractography) was applied for the identification and characterization of microcracks in stone and to determine the relationship of the deposit of the consolidant to the stone substrate.

The lattice preferred orientation (here referred to as texture) of the marbles was determined by means of neutron diffraction (cf. Leiss & Ullemeyer 1999). Due to the high penetration depth of neutrons, large sample volumes may be investigated and a better approximation of the bulk rock texture is achieved.

For a quantitative determination of porosity and pore size distribution mercury porosimetry was used (cf. Brakel *et al.* 1981).

Ultrasonic velocity measurements were used for the detection of marble degradation by thermal treatment on cubic rock samples (65 × 65 × 65 mm). Transient times of ultrasonic pulses were determined (piezoceramic transducers, resonant frequency 1 MHz) in three orthogonal directions using the pulse transmission technique (Birch 1960, 1961). The measurements were performed with dry, completely water-saturated and experimentally impregnated samples.

The thermal expansion behaviour was measured on cuboids (10 × 10 × 50 mm). The directional dependence of the thermal expansion was determined as a function of temperature using a triple dilatometer (cf. Tschegg *et al.* 1999; Siegesmund *et al.* 2000). The final displacement resolution was better than 1 μm. For a detailed description of the experimental setup refer to Widhalm *et al.* (1996). The thermal expansion coefficient α expresses the expansion of a material as a function of temperature. Calcite shows an extremely anisotropic α (Kleber 1959): $\alpha_{11} = 26 \times 10^{-6}\ K^{-1}$ parallel and $\alpha_{22} = \alpha_{33} = -6 \times 10^{-6}\ K^{-1}$ perpendicular to the

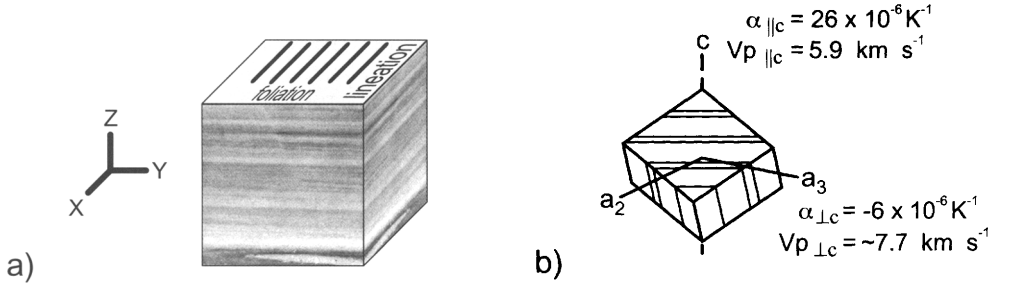

Fig. 1. (**a**) Reference coordinates with respect to foliation and lineation. (**b**) The calcite cleavage rhombohedron together with the values for thermal dilatation (Kleber 1959) and ultrasonic velocities (Dreyer 1974) in the directions of the c- and a-axes of the single crystal.

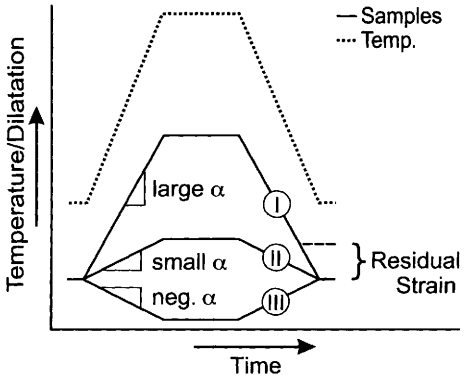

Fig. 2. Curves for different thermal dilatation coefficients α observed in expansion measurements (I = large α, II = small α and III = negative α). Residual strain remains if a sample does not return to its initial length.

crystallographic c-axis (Fig. 1b), i.e. calcite contracts normal to the c-axis and expands parallel to the c-axis during heating. The coefficient of thermal expansion for the investigated marbles was calculated from the experimentally determined temperature and dilatation data ($\alpha = \Delta l/(l \times \Delta T)$). In Figure 2, heating/cooling ramps are schematically shown for a strong (small α), a weak (large α) and a negative thermal dilatation coefficient. All investigations were performed on three mutually perpendicular specimens to gain information on the directional dependence of the data.

Consolidation

The $PMMA_{sol}$ is a specially modified polymethyl-methacrylate with a minor portion of polymethyl-butyl copolymer and some acid groups added for better adhesion (cf. Koblischek 1990). The acrylic resin has a molecular size smaller than 24 nm, the density is about 0.95 g cm^{-3}, and the glass transition temperature (T_g) is approximately 60°C. For the purpose of this investigation it is dissolved in xylenes to a concentration of 40%. The polymer becomes effective after evaporation of the solvent by forming films of varying strength.

The PSAE is an ethylsilicate comprising three to five silicic acid ester molecules. The oligomers have a molecular size between 1.2 and 6 nm with the predominant portion about 3 nm (Koblischek 1990). The PSAE is dissolved in ethanol with an active ingredient content of 40%.

For the $PMMA_{poly}$ approach the rock samples are fully impregnated with monomer methyl-methacrylate and polymerized in situ. The $PMMA_{poly}$ generated by this means is a Plexiglas with a T_g at approximately 85°C and a thermal dilatation coefficient (α) of 70 × 10^{-6} K^{-1}. The impregnation solution also contains an acrylic silane and acrylic acid (Lorenz & Ibach 1999). The volume reduction during the polymerization is approximately 20 vol%.

The first two methods are usually used for on-site consolidation. Both consolidants are normally applied on the rock surface and are incorporated by capillary uptake. To facilitate impregnation, the dissolved consolidants are repeatedly applied with a smaller agent content. In order to gain a complete impregnation of the materials under investigation, the stone consolidants are applied under a vacuum of 0.07 bar followed by a confining pressure up to 6 bar. To provide an interconnecting porosity, the marble samples were thermally preconditioned by heating them up to 200°C. This procedure was not necessary for the sample from Carrara since it was already extremely deteriorated.

The third consolidation method is normally not performed on site. Before impregnation, the rock samples were dried by heating up to approximately 70°C (cf. Lorenz & Ibach 1999). The samples were then placed in a vessel which was introduced in a vacuum/pressure kettle. Under vacuum the vessel was fully filled with monomer methyl-methacrylate. The radical polymerization was initiated at approximately 80°C after some vacuum/pressure stages (0.75/25 bar).

Grain fabrics

Carrara marble

The Carrara marble was taken from the exterior of a strongly weathered window sill from the Marble Palace in Potsdam (Germany). The specimen is of a bright white colour and contains irregular grey veins. The veins are folded and show a streak-like distortion and usually range in width from 0.5 to 2 cm. A preferred orientation of the veins is not clearly detectable. The sample shows a strong decay in the form of granular disintegration.

Microstructurally, the Carrara marble shows a nearly equigranular polygonal grain fabric (Fig. 3a) with straight grain boundaries and 120° triple-point junctions (Fig. 4a). The grain size in the white areas is about 200 μm and the grain size distribution shows a narrow maximum

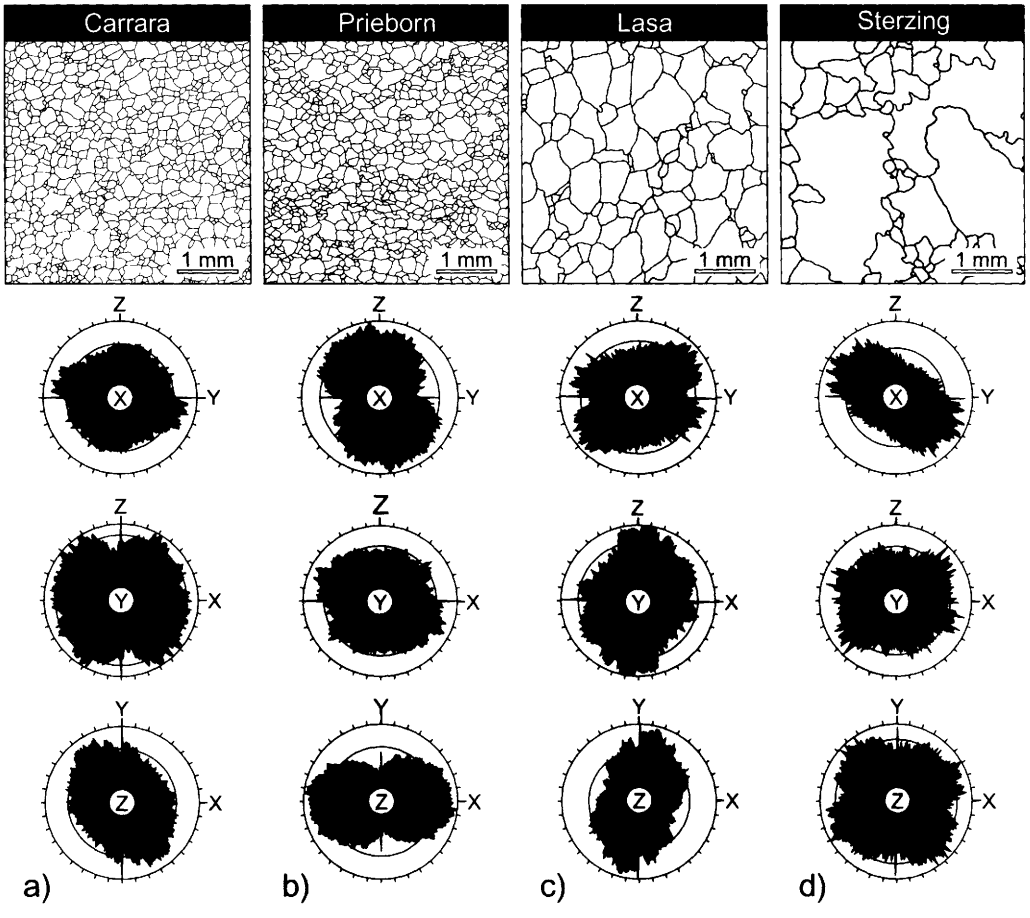

Fig. 3. Results from quantitative image analyses. Top, thin section drawings illustrating the grain fabric and the relative grain size differences (XY-plane). Below, the statistical orientations of grain boundaries are shown in the YZ-, XY-, XZ-plane.

(Fig. 5a). In the XY-plane of the investigated sample a weak preferred grain boundary orientation (subparallel Y-direction) can be observed (Fig. 3a).

The grey veins are fine grained (average grain size = 50 μm) and the grains have a very strong undulose extinction. Grain boundaries are interlobate and a high amount of fluid inclusions or graphite occurs which probably causes the grey colour of the veins.

Prieborn marble

The weathered sample of the Prieborn marble (Poland) was also taken from the Marble Palace and represents an exposed outside staircase. The marble is grey in colour and exhibits a foliation of alternating dark and light grey layers. The start of degradation is observable along the grain boundaries and, in particular, within the superficial layers. However, the state of deterioration is less pronounced than that of the Carrara marble.

The grain fabric is very similar to that of the Carrara marble (Fig. 3b). However, the grain boundaries are slightly more curved or very finely serrated (Fig. 4b). The average grain size is about 200 μm (Fig. 5b) intercalated with fine-grained layers with grain size less than 100 μm. A grain shape preferred orientation of weakly elongated grains can be observed in the YZ-section (||Z-direction) and also in the XY-plane (||X-direction) of the specimen (Fig. 3b).

Twinning rarely occurs, even though a preferred orientation of the lamellae subparallel to the foliation is detectable in the

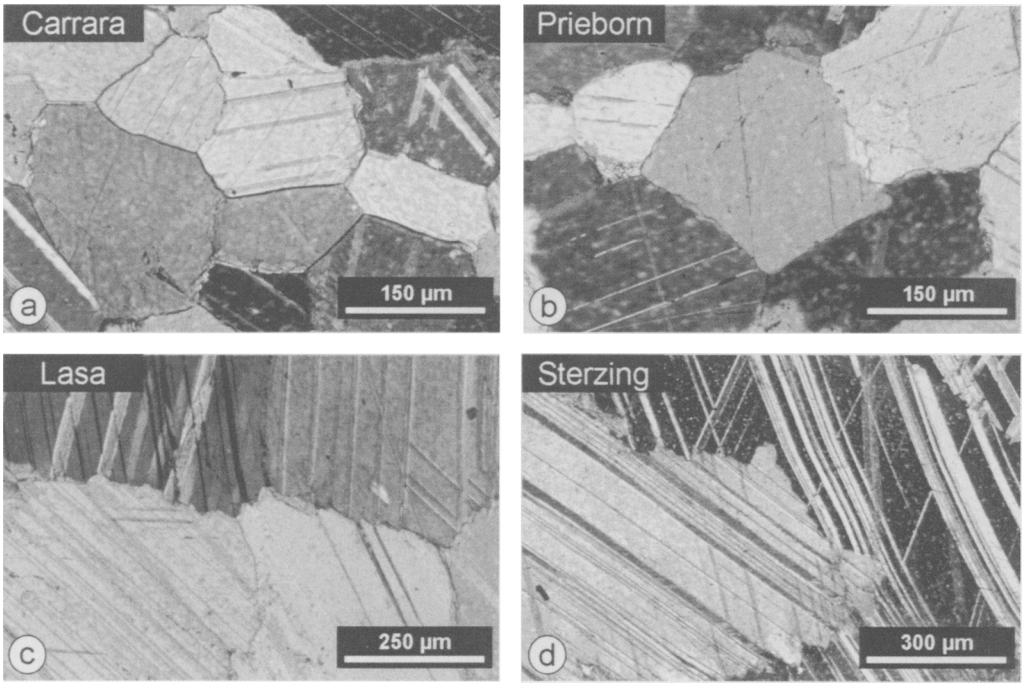

Fig. 4. Photomicrographs (crossed polarizers) showing the grain boundary geometry. The images correspond to the XZ-section.

XZ-section. The grain boundaries are open and decorated with dark material. Together with fluid inclusions, this causes the grey colour of the marble. Small quartz grains and pyrite occur as accessory mineral phases.

Lasa marble

The Lasa sample comes from a replaced grave stone exposed for more than 40 years. Macroscopically the marble shows a bright white colour. Only a few light grey layers about 4 cm wide could be observed marking the foliation. The main weathering feature of this sample is a weak chemical exsolution at the rock surface along grain boundaries and cleavage planes of the calcite crystals.

The grain fabric of the marble is more or less inequigranular (Fig. 3c) and the grain boundary geometry is slightly irregular (Fig. 4c). In contrast to the Carrara and Prieborn marble types, the Lasa sample exhibits a larger average grain size of about 700 µm (Fig. 5c). In all the investigated directions a slight preferred orientation of grain boundaries can be observed which is most evident in the XY-plane (Fig. 3c).

Sterzing marble

This sample was originally used as a grave stone. Macroscopically the marble is characterized by a greyish white colour and a coarser grain size. Superficially, a pronounced chemical exsolution along calcite cleavage planes and grain boundaries is observable.

This marble shows a seriate grain fabric (Fig. 3d). The grains have irregular shapes with strongly curved, interlocking grain boundaries (Fig. 4d). Twinning is more frequent and the grains show undulose extinction, deformation bands, subgrain formation and bent twin lamellae. This fabric is interpreted as the result of a late-stage deformation with the interlocking grain boundaries indicating grain boundary migration (Fig. 3d). Subgrains as well as recrystallized grains along the grain boundaries also reveal a subgrain rotation recrystallization (Passchier & Trouw 1996).

The average grain size is about 1.5 mm (Fig. 5d). The coexistence of large and small grains can only be visualized when the diameters of the grains are shown as a fraction of the total number of grains (Fig. 5d). With respect to the total number of grains, smaller grains show a higher frequency compared with larger ones.

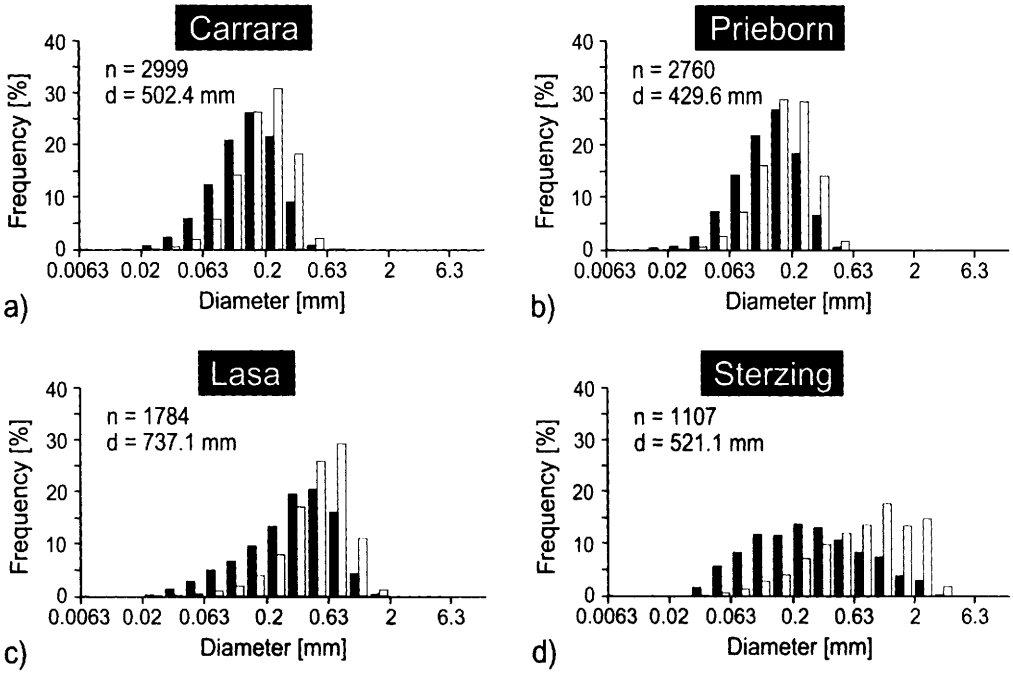

Fig. 5. Grain size distributions determined by quantitative image analysis. The values of the different sections (XY-, YZ-, XZ-plane) have been averaged. The relative frequency of a specific diameter class has been calculated with respect to the total diameter (grey bars; d = total diameter) and to the total number of grains (black bars; n = total number).

A pronounced preferred orientation of grain boundaries is only observable in the YZ-plane and is oblique to the Y-direction (Fig. 3d).

Trails of fluid inclusions are common. Moreover, the sample exhibits biotite flakes on the grain boundaries and within the calcite grains. Quartz is found as an accessory mineral (about 1%), which occurs as small round inclusions in calcite crystals.

Texture

The calcite single crystal has extreme anisotropic properties. Therefore, the texture may have an important influence on the strong directional dependence of physical/mechanical parameters (Widhalm *et al.* 1996; Siegesmund *et al.* 1999).

The marbles in this study show significant differences in their texture. Two general texture types can be defined. The first is observed for the Carrara and the Prieborn marbles and can be described as a c-axis fibre type (Fig. 6a,b). The c-axes form a slightly elongated maximum perpendicular to the foliation, whereas the a-axes show a girdle distribution subparallel to the foliation with a maximum parallel to the X-direction. Although both marbles exhibit similar grain fabrics and also similar texture patterns, the texture strength is different. The Prieborn marble shows a strong c-axis maximum of 3.6 mrd, while the Carrara marble exhibits a maximum of only 2.0 mrd (mrd = multiples of random distribution). The Sterzing marble also shows the characteristics of a c-axis fibre type (Fig. 6d). The Carrara and the Prieborn marbles show a weak girdle distribution of the a-axes, which is more pronounced for the Sterzing marble.

The second texture type can be found in the Lasa marble. The c-axes of this marble show a girdle distribution (Fig. 6c) and the a-axes form a point maximum preferentially orientated parallel to the X-direction. Due to this particular texture type, a different thermal expansion behaviour is expected when compared to the other marbles.

Pore space characteristics of weathered and impregnated samples

Grain boundary cracks and intragranular cracks parallel to cleavage planes and twin lamellae are

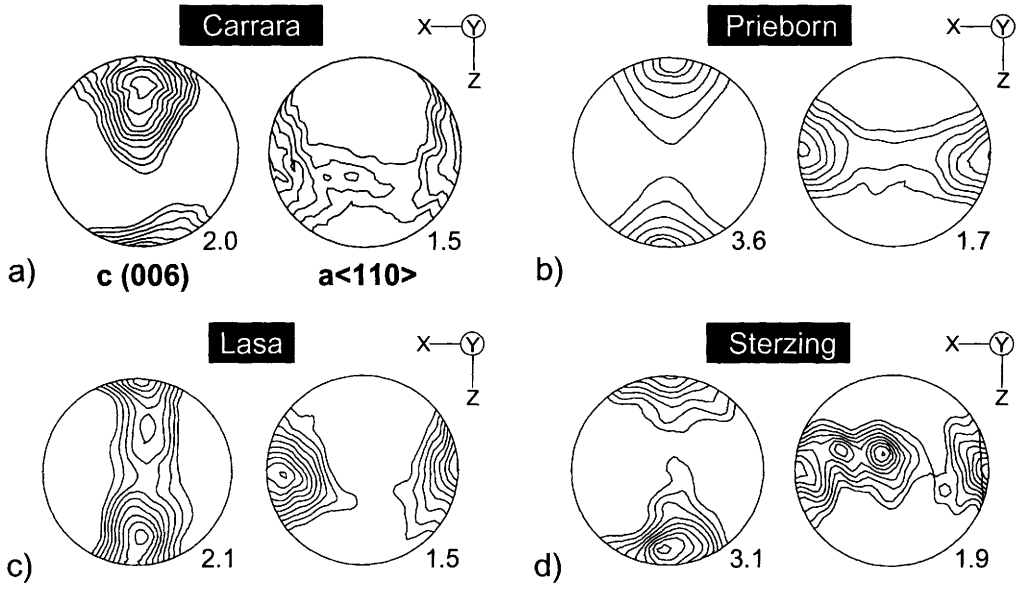

Fig. 6. Texture patterns of the different marbles (lower hemisphere, stereographic projection; lowest contour is equal to 1.0 multiples of random distribution (mrd); the relative maxima are given).

observable in all investigated marble samples. Thus, the pore spaces of the weathered marbles are characterized by a primary crack porosity. The intergranular cracks are found predominantly in the Carrara and Prieborn marbles, and therefore, in fine grained marbles with relatively straight grain boundaries. Intragranular cracks frequently occur in the coarser grained Sterzing marble. The curved, interlocking grain boundary geometry of this marble type leads to an activation of internal planes in the calcite crystals.

Stone consolidants within the pore space

The disposition of stone consolidants within the pore space of the marbles provides important information about the adhesion between calcite and the impregnation material. Evaluations can be made about the modification of the pore space including secondary porosity and its interconnected network.

The $PMMA_{sol}$ consolidated marbles are characterized by locally isolated films in the pore space, detectable by SEM analyses. These isolated films vary in shape and size depending on the marble. In the strongly weathered Carrara marble with its large pore radii these films occur as relatively expanded coatings at grain boundaries (Fig. 7a). These coatings are sporadic and reproduce the relief of the underlying grain boundary topography (Fig. 7b). The $PMMA_{sol}$ films often exhibit holes with irregular shape. The rims of these holes appear rounded and cannot be explained by fracturing, e.g. during sample preparation. They are interpreted as shrinkage phenomena generated during evaporation of the solvent. The size of the films depends on the pore size. The Carrara and Prieborn marbles exhibit large films, while the Lasa and the Sterzing marbles, with relatively small pore sizes, show only isolated small accumulations.

The PSAE occurs as irregular, flat shards, separated by cracks (Fig. 7c). This structure can be attributed to shrinkage after gelation. The individual fragments show a mostly disc-like polygonal shape, and their size varies between approximately 5 and 30 μm. The width of the shrinkage cracks between the shards ranges from 0.5 to 3 μm (Fig. 7d). The fact that all of the PSAE gel remains in place on fractured surfaces, and that there is no negative pattern of cleavage planes and grain boundaries in the gel, indicates little or no cohesion between the gel and the calcite grains.

The $PMMA_{poly}$ appears as relatively dark coatings in the SEM images using the backscattered mode. In contrast to the PSAE consolidant, the negative pattern of cleavage planes on the detached $PMMA_{poly}$ plane is evidence that the cracks were completely filled (Fig. 7e) and

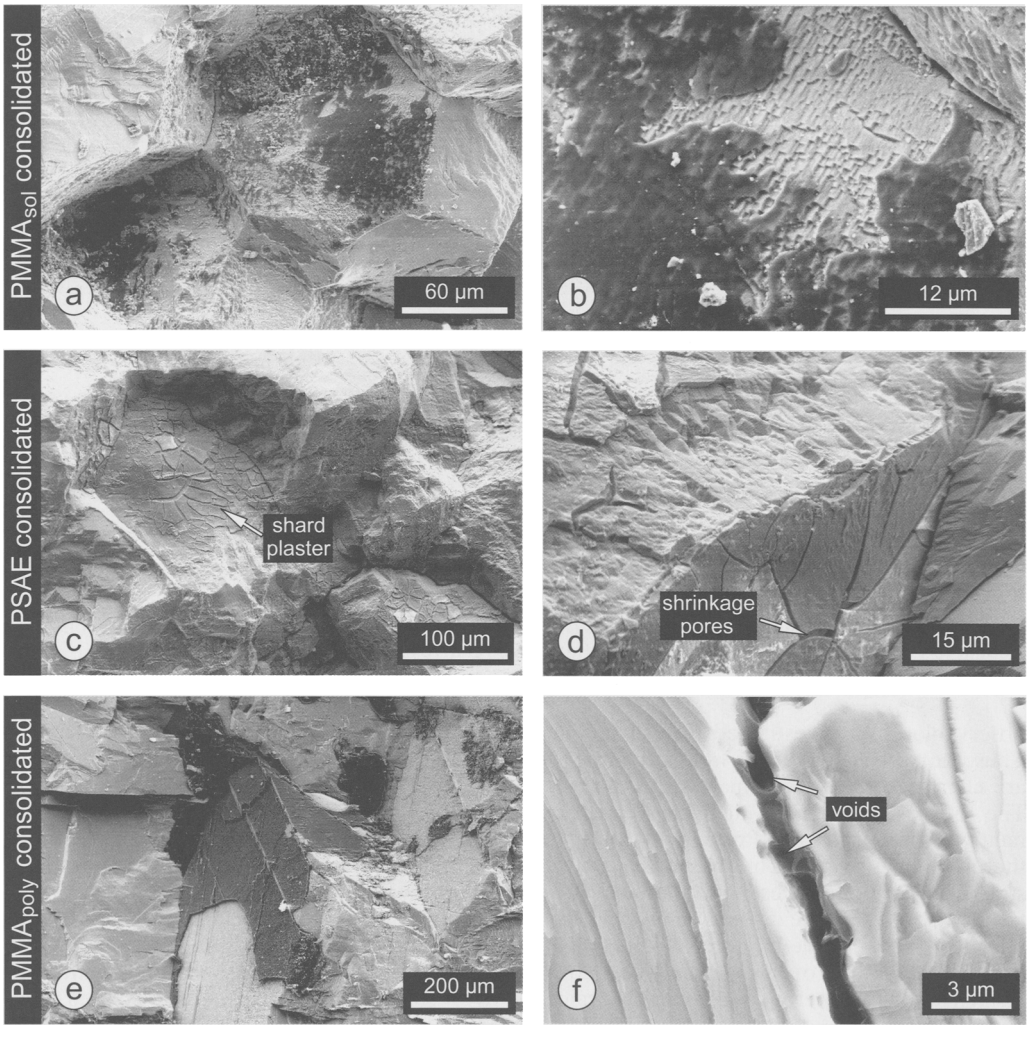

Fig. 7. Backscattered images (SEM) of impregnated specimens (fractography). (**a**–**d**) Consolidated samples of Carrara marble which show a preferred cracking along grain boundaries. (**e**,**f**) Sterzing marble with a preferred degradation along intragranular planes.

that a pronounced cohesion was induced by this consolidation process. In sections perpendicular to the filled cracks, small holes with oval shapes about 1 µm in size are observable. They occur in the central parts of the $PMMA_{poly}$ (Fig. 7f). They are interpreted as voids due to volume reduction of the $PMMA_{poly}$ during polymerization (see also Lorenz & Ibach 1999).

Porosity and pore size distribution

The pore size distribution has been determined for all weathered and impregnated marble samples. The comparison between consolidated and unconsolidated samples gives important clues about sizes of pores preferentially invaded by each consolidant.

As an example of the data obtained for $PMMA_{sol}$ impregnation, the pore size distribution measurements of the Lasa marble are given in Figure 8a,b. For this marble type a porosity reduction of about 40% is observable after $PMMA_{sol}$ impregnation which corresponds to the percentage of active ingredient in the treatment solution. Thus the bulk of the pore volume is filled by this solution.

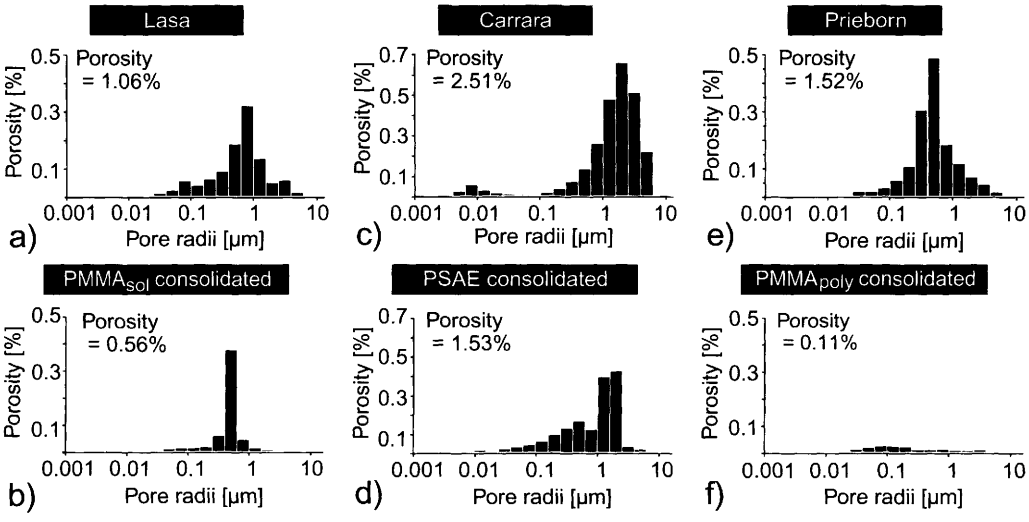

Fig. 8. Modification of the pore size distribution and porosity by consolidation. Data are given for the unconsolidated and consolidated samples of (**a**,**b**) Lasa, (**c**,**d**) Carrara and (**e**,**f**) Prieborn marbles.

The distribution of pore sizes was also clearly modified by impregnation. Whereas the weathered sample shows a broad distribution of pore radii classes around a single maximum from 0.630 µm to 1.000 µm, the majority of the classes of the impregnated sample are strongly reduced. The pore size frequency maximum is shifted by one pore size class downward. This downward shifting of the pore size maximum after impregnation is evident for all samples impregnated with $PMMA_{sol}$.

For the modification of the pore space by PSAE impregnation the Carrara marble will serve as an example (Fig. 8c,d). The weathered sample shows a porosity of 2.51% while the porosity of impregnated specimens is 1.53%. This means a reduction of porosity due to consolidation of approximately 40%. The pore size distribution for the weathered Carrara sample shows a significant maximum in the radius range from 0.630 µm to 6.300 µm and a second, submaximum between 0.004 µm and 0.016 µm (Fig. 8c). The impregnated sample does not exhibit the lower peak (Fig. 8d). This indicates that (i) this pore class was filled by the PSAE (molecular size approximately 3 nm) or (ii) the pores are no longer accessible to mercury. Furthermore, the pore sizes above 1 µm are strongly modified. Pore sizes above 2.512 µm almost completely vanished and a new maximum occurs between 1.000 µm and 2.512 µm. These pore sizes are evident in untreated samples, and therefore become more prominent because other pore sizes are filled. For all samples impregnated with PSAE a comparable behaviour can be observed.

The pore size distributions for the Prieborn marble without and with full impregnation with $PMMA_{poly}$ are shown in Figure 8e,f. The porosity is reduced from 1.52% in the weathered sample to 0.11% in the impregnated specimen. This reduction of approximately 93% is higher than the expected reduction of about 80% by volume reduction due to polymerization. Thus, the majority of the voids created by polymerization are not accessible to mercury.

The pore size distribution of the weathered sample shows a strong maximum in the range from 0.159 µm to 1.585 µm and the distribution for the impregnated sample shows that almost all pores are closed (Fig. 8f). Only a few pores with a size of about 0.100 µm are still present.

Thermal dilatation

The thermal dilatation measurements were performed using four heating cycles up to 42°C, 65°C and 90°C with a heating rate of about 1°C min^{-1}. The third cycle up to 90°C was repeated to verify if the samples show a modified behaviour. The maximum temperature (T_{max}) was held for 60 min permitting thermal equilibration of the specimens. After each cycle the samples were cooled to the initial temperature of about 25°C.

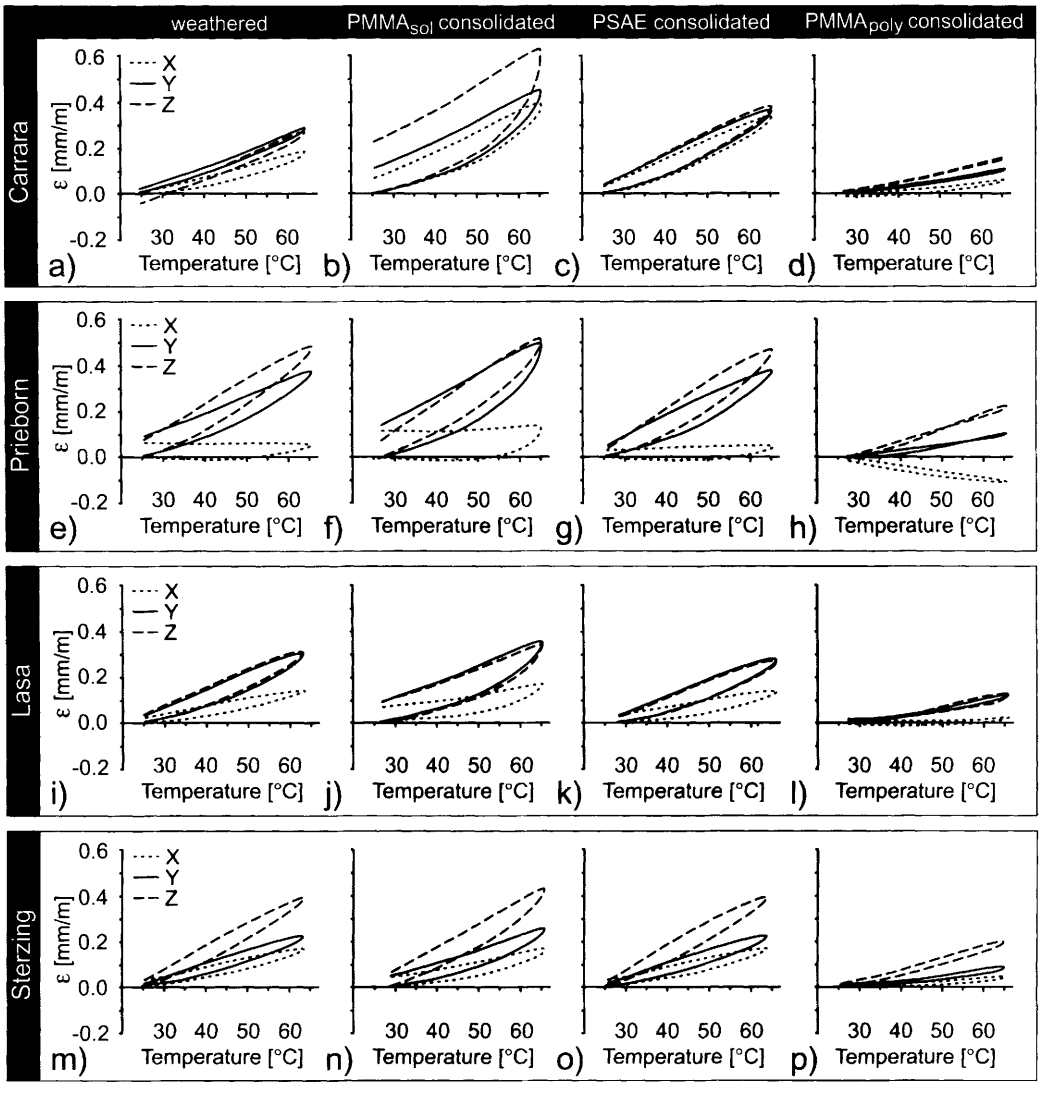

Fig. 9. Experimentally determined thermal dilatation as a function of heating up to 65°C for weathered and consolidated marbles. The dilatation curves are given for the X-, Y- and Z-direction.

The calcite single crystal coefficients of thermal dilatation can be treated as linear because the temperature interval at a maximum $\Delta T = 65°C$ used for the dilatation experiments is insignificant. Thus, the thermal dilatation ε (mm m^{-1}) observed in the experiments should be closely linked to the texture strength of the respective sample.

The different marbles show a more or less pronounced directional dependence of thermal dilatation. This is a well known phenomenon (Widhalm *et al.* 1996; Tschegg *et al.* 1999; Siegesmund *et al.* 2000) and can be attributed to the anisotropic expansion behaviour of the calcite single crystal (see Fig. 1b) in conjunction with a lattice preferred orientation (texture; see Fig. 6a–d). Furthermore, the intensity for directional dependence of consolidated and weathered samples is comparable for the respective marble types.

The anisotropy of thermal dilatation for the Prieborn and Lasa marbles will serve as an example in the discussion on the effect of texture (Fig. 9e,i). The thermal dilatation of the

Table 1. *Residual strains $\Delta\varepsilon$ (mm m^{-1}) for weathered and consolidated Carrara and Prieborn marbles as a result of heat treatment*

	Direction	Cycle 42°C	Cycle 65°C	Cycle 90°C	Cycle 90°C
Carrara marble					
Weathered	X	0.000	0.000	0.000	0.000
	Y	0.000	0.000	0.000	0.000
	Z	−0.071	−0.047	−0.055	−0.032
$PMMA_{sol}$	X	0.000	0.063	0.111	0.000
	Y	0.000	0.108	0.057	0.000
	Z	0.040	0.225	0.181	0.000
PSAE	X	0.021	0.027	0.049	0.000
	Y	0.000	0.039	0.056	0.000
	Z	0.000	0.039	0.059	0.000
$PMMA_{poly}$	X	0.000	0.000	0.150	0.043
	Y	0.000	0.000	0.159	0.034
	Z	0.000	0.000	0.102	0.000
Prieborn marble					
Weathered	X	0.000	0.054	0.099	0.000
	Y	0.027	0.086	0.134	0.000
	Z	0.042	0.066	0.094	0.000
$PMMA_{sol}$	X	0.000	0.116	0.085	0.000
	Y	0.032	0.141	0.095	0.000
	Z	0.000	0.074	0.030	0.000
PSAE	X	0.000	0.027	0.047	0.000
	Y	0.000	0.052	0.055	−0.026
	Z	0.035	0.045	0.042	0.000
$PMMA_{poly}$	X	0.000	0.000	0.141	0.031
	Y	0.000	0.000	0.185	0.026
	Z	0.000	0.000	0.128	0.000

Prieborn sample parallel to the Z-direction (parallel to the c-axis maximum, cf. Fig. 6b) is larger than the expansion parallel to the X-direction (parallel to the a-axis maximum, cf. Fig. 6b). The expansion parallel to the Y-direction represents an intermediate direction. This expansion behaviour is typical for c-axis fibre type marbles (Leiss & Weiss 2000). In contrast, the texture of the Lasa sample represents an a-axis fibre type (Fig. 6c). Thus, the thermal expansion (ε) shows nearly identical values for the Y- and Z-direction controlled by the girdle distribution of the c-axis (see Fig. 6c). The lowest ε is observed parallel to the a-axis maximum (X-direction).

The texture strength is also evidenced in the expansion behaviour of the samples. The Carrara marble with a relatively weak c-axis maximum of 2.0 mrd shows only a small anisotropy, whereas the Prieborn marble with a c-axis maximum of 3.6 mrd has a stronger directional dependence of thermal dilatation ε.

A permanent expansion (residual strain; cf. Battaglia *et al.* 1993; Siegesmund *et al.* 2000) is well documented by the thermal expansion of the X-direction of the Prieborn marble (Fig. 9e). This direction corresponds to the maximum of the a-axis concentration, i.e. the direction of the negative single crystal thermal dilatation coefficient. Due to the strong texture of this specimen, a contraction with increasing temperature can be predicted from the texture, and is demonstrated by the experimental results shown in Figure 9e for the temperature range up to 45°C. Above 45°C the thermal dilatation reaches positive values. After heat treatment the residual strain of the specimen is similar in extent to the observed maximum of dilatation (Fig. 9e).

In the following section the thermal dilatation behaviour is summarized with respect to the ramps. The curves for a maximum temperature of 65°C are shown in Figure 9a–p while residual strains are given in Table 1.

The thermal dilatation behaviour for unconsolidated samples during the first heating cycle up to 42°C shows a more or less linear expansion, whereas no residual strain remains. Only for the Z-direction of the Carrara marble does a contraction occur. This behaviour observed in the Carrara marble holds for all applied cycles (cf. Table 1), and is interpreted as

a fabric collapse due to its advanced decay pattern.

For cycles up to 65°C the Lasa and Sterzing marble (Fig. 9i,m) exhibit a slight increase of thermal dilatation above 40°C resulting in a weak residual strain. The same behaviour occurs for the Prieborn marble, whereas the permanent length change after cooling is more pronounced (Fig. 9c; cf. Table 1).

The heating cycle up to 90°C leads to a stronger non-linearity of the curves and a more or less pronounced residual strain. Again, the Prieborn marble shows the highest values, and therefore the strongest thermal degradation (cf. Table 1).

The largest residual strain for the Prieborn marble occurs parallel to the Y-direction, since many other investigated marble types show the main residual strain parallel to the c-axis maximum (Siegesmund *et al.* 2000). However, image analyses reveal that a preferred orientation of grain boundaries in the XZ-plane exists (see Fig. 3b) causing a preferred crack propagation in this direction. Since this marble shows a thermal degradation along grain boundaries, their preferred orientation could be the cause for the preferred crack propagation in the XZ-plane.

The second heating cycle up to 90°C was performed in order to prove whether the thermal degradation is linked only to the maximum temperature or to the differential temperatures. In the first case, the residual strain should be vanishingly small and in the second case, the residual strain should be as large as that observed for the first 90°C cycle. For all samples, the residual strain observed for the second 90°C cycle is vanishingly small (cf. Table 1). Thus, the main damage takes place between 40°C and 90°C.

Consolidated samples

The $PMMA_{sol}$ impregnated marble samples show a distinct modified thermal behaviour especially for cycles of higher temperatures. By heating the $PMMA_{sol}$ consolidated samples up to 42°C a relatively linear thermal expansion is observed and, correspondingly, no residual strain remains (Fig. 10a). Only the Z-direction of the Carrara marble and the Y-direction of the Prieborn marble show a slight residual strain after heat treatment (Table 1) indicating that the directions of strongest thermal degradation were preferentially activated after consolidation.

By heating the $PMMA_{sol}$ consolidated marbles up to 65°C (especially for the Prieborn and Carrara marbles) the slope of the curves, and thus the thermal expansion coefficients increase when the temperature transcends 50°C (Figs 9b,f and 10b). Both samples exhibit a large residual strain after heat treatment in all directions, which is significantly larger than the residual strain of the respective non-impregnated specimens. This effect can be attributed to a weakening of the resin when approaching its glass transition temperature (T_g = approximately 60°C). The amount of residual strain indicates that (i) new cracks are generated or (ii) the PMMA is stretched. For the Lasa and Sterzing samples a comparable expansion behaviour is observable, whereas a smaller residual strain occurs (Fig. 9h,j), resulting from the small initial degradation.

For the $PMMA_{sol}$ impregnated Carrara marble a large directional dependence of thermal dilatation and of the residual strain is observed (Fig. 9b). The effect of $PMMA_{sol}$ is different in several directions, which can be explained by the preferential orientation of the system of cracks.

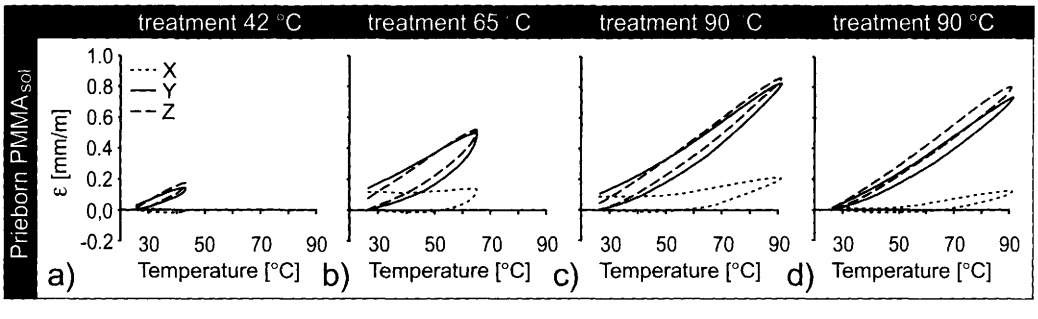

Fig. 10. Thermal dilatation curves of heating cycles up to (**a**) 42°C, (**b**) 65°C (**c**) 90°C and (**d**) 90°C for the Prieborn marble consolidated with $PMMA_{sol}$.

The dilatation behaviour of the samples by the first heating up to 90°C is characterized by a slight increase of the hysteresis loop above approximately 50°C (cf. Fig. 10c). A pronounced residual strain is found only for the Carrara and Prieborn marbles, but it is lower than the observed change in length for the heating cycle up to 65°C. The only exception is represented by the X-direction of the Carrara marble (Table 1) because a larger residual strain remains. For the second heating cycle up to 90°C no further residual strain occurs (cf. Table 1), while the hysteresis follows a more linear trend (see for example the Prieborn marble in Fig. 10d).

The PSAE consolidated samples show only minor changes compared with non-impregnated specimens (Fig. 9c,g,k,o). For the heating cycle up to 42°C the thermal dilatation is more or less linear. Also, no significant residual strain remains after treatment. A slightly increased residual strain is seen only for the X- and Z-direction of the Carrara and the Prieborn marbles, respectively (Table 1).

The dilatation scenario for the second cycle up to 65°C is only slightly modified, except for the Carrara marble (Fig. 9c). In contrast to the unconsolidated Carrara sample, no contraction is observed parallel to the Z-direction and the maximum expansion is slightly increased. The observations indicate that the PSAE in the pore space has stabilized the grain fabric.

For the first heating up to 90°C all PSAE-consolidated samples show a slight increase of dilatation and a weak residual strain (Table 1).

The small modifications induced by PSAE impregnation probably originated by a low thermal expansion coefficient in these materials. Furthermore, no structural changes of the PSAE can be observed such as determined for the PMMA resins (glass transition temperature).

For the $PMMA_{poly}$ consolidated marbles and heating cycles up to 42°C and up to 65°C a very similar behaviour occurs. This consolidation method generates the most conspicuous change of thermal expansion behaviour. All samples show a pronounced reduction of thermal dilatation and a change of the elastic behaviour after impregnation. This is shown by the strong modification of the hysteresis loops (Fig. 9d,h, l,p), i.e. the curves are very linear. For the Prieborn marble parallel to the X-direction a pronounced contraction can be observed (Fig. 9h). The contraction direction is coincident with the preferred orientation of the a-axis. This can be attributed to the adhesion generated by $PMMA_{poly}$ consolidation, which leads to a stronger transfer of the single crystal properties in the whole rock. Furthermore, for all samples of $PMMA_{poly}$ consolidation no residual strain remains for the heating cycles up to 42°C and up to 65°C (Table 1).

Only when the $PMMA_{poly}$ consolidated samples were heated up to 90°C did the thermal dilatation behaviour change significantly. This is characterized by a surge of thermal dilatation around 80°C (Fig. 11). After cooling to the initial temperature a pronounced residual strain also remains. The experimentally determined

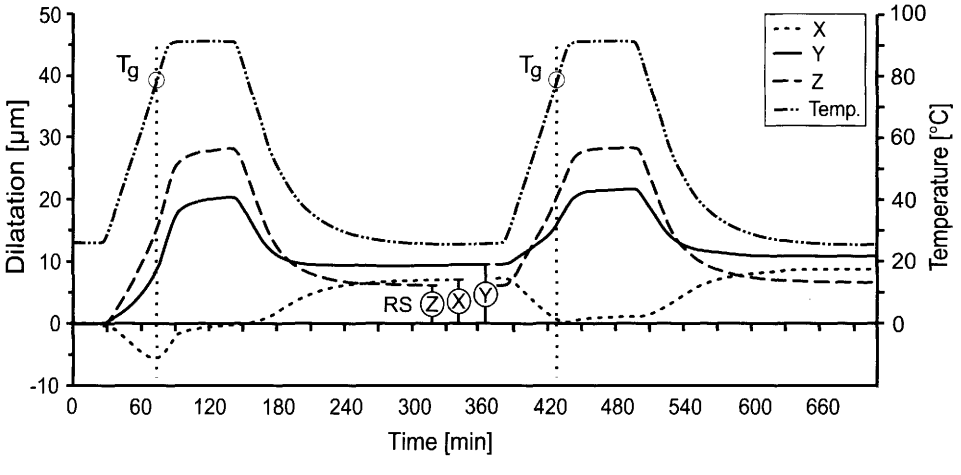

Fig. 11. Dilatation curves of two heating cycles for treatment up to 90°C of a $PMMA_{poly}$ consolidated Prieborn marble. RS = residual strain, as given for all directions after the first heating cycle.

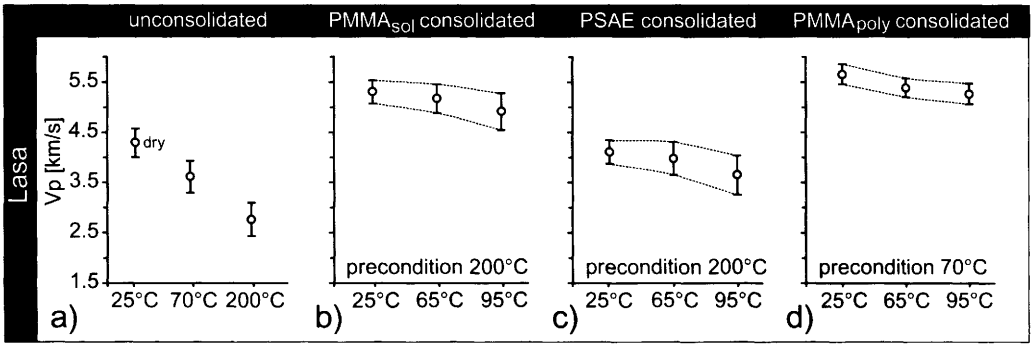

Fig. 12. Experimentally determined ultrasonic velocities (V_p) for the Lasa marble. Values are given for different sample conditions: (**a**) dry and pre-conditioned by heating the samples up to 70°C and 200°C; (**b–d**) consolidated and thermally treated up to 65°C and 90°C.

temperature for a significant change of the material coincides with the glass transition temperature of the PMMA$_{poly}$ used.

For the second heating cycle up to 90°C the transition point is only weakly developed (Fig. 11). Nevertheless a measurable residual change in length can be determined for most samples (cf. Table 1).

Ultrasonic wave velocities

A method for determining the state of deterioration and of the improvement by consolidation is by measuring the velocities of ultrasonic waves through the samples, i.e. of compressional waves (V_p). This method is efficient, quick and non-destructive (Snethlage *et al.* 1999). The basic principle is that the magnitude of the rock degradation is monitored by decreasing V_p (cf. Weiss *et al.* 2000). Inversely, the velocities should increase by cohesion re-establishment (cf. Snethlage *et al.* 1999).

The velocity data observed for weathered and consolidated Lasa marble are shown in Figure 12a–d as an example, but the same relationships apply to the other marbles. For dry samples the velocities range from 4.0 to 4.6 km s^{-1}. Before consolidation, the specimens were heated up to 70°C (PMMA$_{poly}$) or 200°C (PMMA$_{sol}$ and PSAE). The corresponding velocity reduction as a consequence of thermal degradation is about 0.7 km s^{-1} by the 70°C heating and 1.5 km s^{-1} by the 200°C heating (see Fig. 12a). These velocities have to be treated as the initial condition of the specimens before consolidation.

The velocity data in the initial stage after consolidation (25°C) are given in Figure 12b,c,d for the different consolidation approaches. All impregnated samples show an increase of ultrasonic velocities, although significant differences occur for the respective consolidation materials.

PSAE consolidation results in a relatively weak increase of ultrasonic velocities of about 1.4 km s^{-1} (Fig. 12c). In contrast, PMMA$_{sol}$ and PMMA$_{poly}$ exhibit a more pronounced change of velocities (Fig. 12b,d). The velocities increased at approximately 2.5 and 2.1 km s^{-1} respectively. The other marbles show a similar pattern of increases of ultrasonic velocities. After heating cycles up to 65°C and 95°C which are comparable with the cycles applied for the dilatation measurements, the ultrasonic velocities for all samples show a slight reduction (Fig. 12c,d). However, the slight reduction of ultrasonic velocities is in the range of resolution of this method.

Discussion

The porosimetry analyses verified that significant differences exist between the investigated marbles in their initial (weathered) stage. For example, the Carrara marble shows a strong deterioration with a sugar-like crumbling of the rock surface. In contrast, the Prieborn, Lasa and Sterzing marbles are less deteriorated which is evident by an initial porosity of less than 1%. However, their weathering histories are different which makes comparison difficult. Observations from the Marmorpalais in Potsdam (Germany) have shown that the Prieborn marble exhibits similar weathering properties to the Carrara marble (Ruedrich *et al.* 2001*a*). Both marble types are characterized by a sugar-like crumbling, indicating a degradation along the grain boundaries. Thus, the main difference between the marble samples is

essentially the weathering intensity rather than the deterioration mechanism.

Magnitude and directional dependence of thermal behaviour frequently coincide with the texture of a marble, i.e. the residual strain is largest parallel to the preferred orientation of the c-axes (Siegesmund *et al.* 2000). However, marbles can exhibit c-axis maxima as well as girdle distributions (e.g. Lasa marble) and the texture strength may vary. Since grain boundary cracking is the predominant type of degradation in marble, a preferred orientation of grain boundaries also leads to an anisotropic distribution of the thermal degradation. Thus, a certain amount of anisotropy in both the thermal expansion coefficient and the residual strain is a general property of all marbles (e.g. Widhalm *et al.* 1996). Consolidation of a marble with a preferred crack system results in an anisotropic distribution of the consolidant. Since the consolidation material has a more or less pronounced effect on the thermal dilatation behaviour, a directional dependence has to be expected for the consolidation.

The consolidation of a porous material leads inevitably to a modification of the pore space, e.g. reduction of porosity and a shift of effective pore radii. Furthermore, secondary effects by gel segregation or curing generates a new pore geometry, e.g. shrinkage cracks in PSAE and $PMMA_{sol}$, voids in $PMMA_{poly}$. Consequently, the interconnectivity is changed and thus other physical parameters of the impregnated marbles, e.g. the water uptake behaviour, should be significantly changed.

The PSAE approach does not improve the cohesion between the grains significantly (see also Goins *et al.* 1996). This effect is evident in the SEM analyses as well as in the relatively small increase of ultrasonic velocities. Furthermore, the thermal behaviour is only slightly modified due to consolidation. However, a PSAE consolidation can stabilize the microstructure of strongly weathered marbles and subsequent impregnation with a cohesion-reinforcing consolidant is possible.

An improved bonding between the grains was generally observed for both PMMA consolidants. This was verified qualitatively by fractography and quantitatively by a pronounced increase of the ultrasonic wave velocities (Fig. 12b,d). However, the expansion behaviour was strongly modified near the specific glass transition temperatures of the two PMMA consolidants. When the temperature reaches the T_g of the respective PMMA consolidants, a significant residual strain occurs (see Table 1). A small decrease in ultrasonic velocity suggests that this residual strain is not unequivocally linked to thermal degradation, but more evidently to a change of the consolidant behaviour from more elastic to more plastic.

A clear change in the dilatation curves after $PMMA_{poly}$ consolidation proves that a significant change in the material's properties occurs. A pronounced reduction of thermal expansion and a significant increase in ultrasonic velocity indicate a good bonding between the calcite surfaces and the $PMMA_{poly}$. However, the extreme reduction of thermal expansion is difficult to understand. Even if the thermal expansion coefficient of polymerized MMA is about $\alpha = 70 \times 10^{-6}\ K^{-1}$, the volume of $PMMA_{poly}$ which invaded the pore space of the marbles is too small for a measurable decrease of dilatation. Thus, the observed reduction of dilatation is possibly caused by a good bonding between the calcite surfaces and the reduction in pore space.

All natural stones from a quarry contain a certain amount of microcracks as a consequence of their complex geological history. Furthermore, weathering causes an increase in pore space. This pore space obviously accommodates a certain part of sample expansion (buffering) until it is closed (cf. Ruedrich *et al.* 2001*b*). $PMMA_{poly}$ impregnation leads to a strong porosity reduction, and thus the buffering vanishes. The final result is a compound material, while the other consolidants do not show this effect. Since strongly anisotropic marbles can show a contraction even after $PMMA_{poly}$ consolidation, the changed thermal expansion behaviour has to be considered for preservation concepts. Furthermore, a difference in thermal behaviour between consolidated and unconsolidated components has to be expected.

In the field, marbles are subjected to numerous temperature changes (e.g. day–night cycles). From the laboratory experiments it is obvious that the thermal degradation of a marble vanishes once a certain temperature is reached. Subsequent cycles at the same temperature result in a significantly reduced or no residual strain. However, on-site the marbles are generally subjected to water, which may reinforce the dilatation and lead to the steady progress of rock damage (Grimm 1999).

Conclusions

The microstructure, the state of preservation and the type of consolidant used are competing parameters determining the thermoelastic properties of a marble. Based on the present

investigation the following conclusions can be drawn.

Thermal degradation of marble depends not only on the texture, but also on the shape fabric of the respective marble. Thus, a complete three-dimensional fabric characterization is indispensable for a quality assessment of marble and associated preservation purposes.

Consolidation of marble using $PMMA_{sol}$, $PMMA_{poly}$ and PSAE changes its thermoelastic properties, since either a consolidation or a stabilization of weathered marbles is observed. The most drastic change is observed for $PMMA_{poly}$. However, the change in the thermoelastic properties varies. Both PMMA consolidants lead to an increase in cohesion between the grains while PSAE stabilizes the microstructure by simply reducing the porosity.

All consolidants reduce the porosity. $PMMA_{sol}$ and PSAE treated marbles show a decrease in porosity and pore radius size according to their agent content, whereas for $PMMA_{poly}$ the porosity almost completely vanishes. Furthermore, other physical properties important for weathering like water absorption will be changed as well after impregnation.

A reinforced cohesion between the grains due to impregnation can be monitored by ultrasonic wave velocity measurements. Both PMMA consolidants show a significant increase in ultrasonic wave velocities after treatment, whereas this effect is limited for PSAE. Therefore, ultrasonic wave velocities seem to be the proper tool for quantifying the effect of consolidation.

After passing the glass transition temperature, a residual strain is observed in thermal dilatation measurements. This does not necessarily coincide with a deterioration, since ultrasonic wave velocities do not show a drastic decrease in thermally treated consolidated marbles.

We are grateful to H. W. Ibach and P. J. Koblischek for their help with the consolidants. Thanks go to G. Wheeler, R. Snethlage and U. Lindborg for their comments. Our work was supported by the Deutsche Bundesstiftung Umwelt and a Heisenberg fellowship from the Deutsche Forschungsgemeinschaft (Si 438/10-1,2 and Si 438/13-1).

References

BATTAGLIA, S., FRANZINI, M. & MANGO, F. 1993. High sensitivity apparatus for measuring linear thermal expansion: preliminary results on the response of marbles. *Il Nuovo Cimento*, **16**, 453–461.

BIRCH, F. 1960. The velocity of compressional waves in rocks up to 10 kilobars, Part I. *Journal of Geophysical Research*, **65**, 1083–1102.

BIRCH, F. 1961. The velocity of compressional waves in rocks to 10 kilobars, Part 2. *Journal of Geophysical Research*, **66**, 2199–2224.

BRAKEL, J. VAN, MODRY, S. & SVATA, M. 1981. Mercury porosimetry: State of the art. *Powder technology*, **29**, 1–12.

CLIFTON, J. R. 1980. *Stone Consolidating Materials – A Status Report*. US Department of Commerce, National Bureau of Standards, NBS Technical Note 1118:46.

DREYER, W. 1974. *Materialverhalten anisotroper Festkörper: Thermische und elektrische Eigenschaften*. Springer, Wien.

DUYSTER, J. 1991. *Strukturgeologische Untersuchungen im Moldanubikum (Waldviertel, Österreich) und methodische Untersuchungen zur bildanalytischen Gefügequantifizierung von Gneisen*. PhD thesis, Göttingen, Geology.

GOINS, E. S., WHEELER, G. S. & WYPYSKI, M. T. 1996. Alkoxysilane film formation on quartz and calcite crystal surfaces. *Proceedings 8th International Congress on Deterioration and Conservation of Stone*, Berlin, 1255–1264.

GRIMM, W. D. 1999. Observations and reflections on the deformation of marble objects caused by structural breaking-up. *Zeitschrift Deutsche Geologische Gesellschaft*, **150**, 195–236.

KESSLER, D. W. 1919. *Physical and chemical tests on the commercial marbles of the United States*. Technology papers of the Bureau of Standards, No. 123.

KLEBER, W. 1959. *Einführung in die Kristallographie*. VEB Verlag Technik, Berlin.

KOBLISCHEK, P. J. 1990. Protection of surfaces of natural stone and concrete through polymers. *In*: MEGUID, S. A. (ed.) *Surface Engineering*. Elsevier Applied Science, 62–71.

LEISS, B. & ULLEMEYER, K. 1999. Texture characterisation of carbonate rocks and some implications for the modeling of physical anisotropies, derived from idealized texture types. *Zeitschrift Deutsche Geologische Gesellschaft*, **150**, 259–274.

LEISS, B. & WEISS, T. 2000. Fabric anisotropy and its influence on physical weathering of different type of Carrara marbles. *In*: LEISS, B., ULLEMEYER, K. & WEBER, K. (eds) *Textures and physcial properties of rock. Journal of Structural Geology*, Special Issue, **22**, 1737–1745.

LORENZ, H. G. & IBACH, H. W. 1999. Marble conservation by Ibach-Total-Impregnation Process: Quality control and optimisation by microscopic and petrophysical data. *Zeitschrift Deutsche Geologische Gesellschaft*, **150**, 397–406.

PASSCHIER, C. W. & TROUW, R. A. J. 1996. *Microtectonics*. Springer, Berlin.

RUEDRICH, J., SIEGESMUND, S. & RICHTER, D. 2001*a*. Marble columns and their state of weathering: structural evidences and ultrasonic tomography. *Zeitschrift Deutsche Geologische Gesellschaft*, **152**, 665–680.

RUEDRICH, J., WEISS, T. & SIEGESMUND, S. 2001*b*. Deterioration characteristics of marbles from

the Marmorpalais Potsdam (Germany): a compilation. *Zeitschrift Deutsche Geologische Gesellschaft*, **152**, 637–664.

SAGE, J. D. 1988. Thermal microfracturing of marble. *In*: MARINOS, P. & KOUKIES, G. (eds) *Engineering Geology of Ancient Works*, Balkema, Rotterdam, 1013–1018.

SIEGESMUND, S., VOLLBRECHT, A., ULLEMEYER, K., WEISS, T. & SOBOTT, R. 1997. Application of geological fabric analyses for the characterization of natural building stones – case study Kauffung marble (in German). *International Journal for Restoration of Buildings and Monuments*, **3**, 269–292.

SIEGESMUND, S., WEISS, T., VOLLBRECHT, A. & ULLEMEYER, K. 1999. Marble as a natural building stone: rock fabrics, physical and mechanical properties. *Zeitschrift Deutsche Geologische Gesellschaft*, **150**, 237–257.

SIEGESMUND, S., ULLEMEYER, K., WEISS, T. & TSCHEGG, E. K. 2000. Physical weathering of marbles caused by anisotropic thermal expansion. *International Journal of Earth Science*, **89**, 170–182.

SNETHLAGE, R., ETTL, H. & SATTLER, L. 1999. Ultrasonic measurements on PMMA-impregnated marble sculptures. *Zeitschrift Deutsche Geologische Gesellschaft*, **150**, 387–396.

TSCHEGG, E. K., WIDHALM, C. & EPPENSTEINER, W. 1999. Reasons for insufficient shape stability of marble plates. *Zeitschrift Deutsche Geologische Gesellschaft*, **150**, 283–297.

WEISS T., SIEGESMUND, S. & RASOLOFOSAON, P. N. J. 2000. The relationship between deterioration, fabric, velocity and porosity constraint. *Proceedings 9th International Congress on Deterioration and Conservation of Stone*, Venice, 215–223.

WIDHALM, C., TSCHEGG, E. K. & EPPENSTEINER, W. 1996. Anisotropic thermal expansion causes deformation of marble cladding. *Journal of Performance of Constructed facilities*, **10**, 5–10.